

CHAPTER IV

RESULTS AND DISCUSSION

4.1 Characterization of *N*-trimethyl Chitosan Chloride (TMC)

4.1.1 Fourier-Transformed Infrared Spectrophotometer (FT-IR)

The functional groups of TMC were investigated by using FTIR spectroscopy. Fig. 4.1 shows the FTIR spectra of chitosan and TMC. Fig. 4.1a represents the basic characteristic peaks of chitosan at : 3446 cm^{-1} (O–H stretch), 2885 cm^{-1} (C–H stretch), 1596 cm^{-1} (N–H bend), 1153 cm^{-1} (bridge–O stretch), and 1094 cm^{-1} (C–O stretch) (Lu *et al*, 2007). Fig. 4.1b shows the new characteristic absorption peaks of TMC spectrum that peak appeared at 1472 cm^{-1} (Chang *et al*, 2009) which is attributed to the methyl groups ($-\text{CH}_3$) of the ammonium, indicating the existence of $-\text{N}(\text{CH}_3)_2$ and $-\text{N}^+(\text{CH}_3)_3$ groups in TMC. The peak of hydroxyl and secondary hydroxyl groups between 960 and 1200 cm^{-1} which found in both chitosan and TMC were not changed that confirm the lack of alkyl groups at C-3 and C-6 in the chitosan.

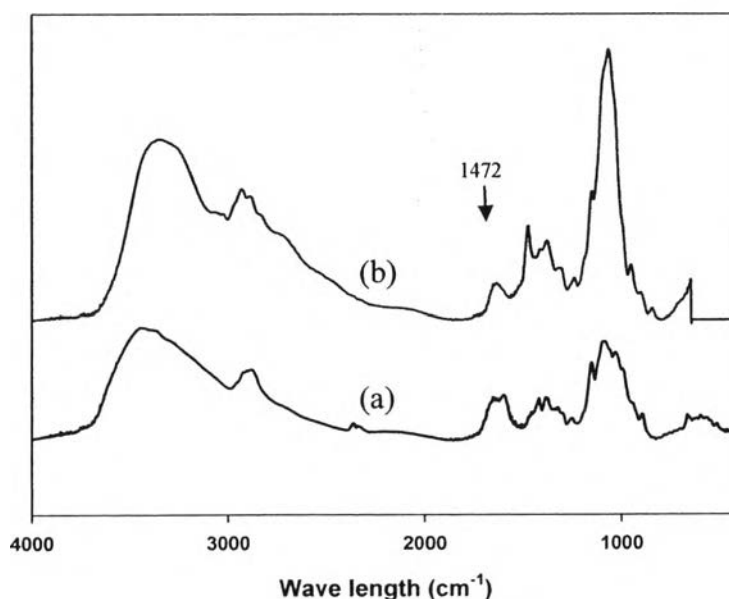


Figure 4.1 The FTIR spectra of : (a) chitosan and (b) TMC.

4.1.2 Proton Nuclear Magnetic Resonance Spectrometer (^1H NMR)

^1H NMR analysis is used to investigate the functional groups and structures of TMC. Moreover, this technique is used to determine the degree of quaternization of TMC. Fig. 4.2 shows the ^1H NMR spectrum of chitosan and TMC. Proton assignment of chitosan was: $\delta_{1.82} = \text{CH}_3$ (acetyl groups); $\delta_{2.90} = \text{CH}$ (carbon 2 of sugar); $\delta_{3.1-3.4} = \text{CH} + \text{CH}_2$ (carbon 3-6 of sugar); and $\delta_{3.66} = \text{CH}$ (carbon of sugar) (Pang *et al.*, 2007). Proton assignment of TMC was: $\delta_{1.87} = \text{CH}_3$ (acetyl groups); $\delta_{2.69} = \text{CH}$ (carbon 2 of sugar); $\delta_{2.89} = -\text{N}(\text{CH}_3)_2$ (dimethyl ammonia); $\delta_{3.16} = -\text{N}^+(\text{CH}_3)_3$ (trimethyl ammonium); and $\delta_{4.94} = \text{H-1}$. The degree of quaternization (DQ) is about 33.79 % and the degree of di-methylation (DM) is about 83.12 % (Chang *et al.*, 2009). These were calculated according to the following equation:

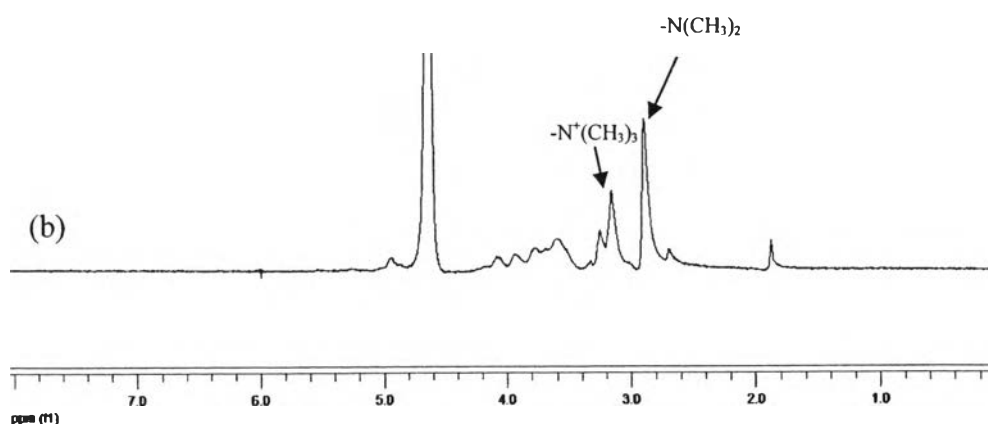
$$DQ = \left[\frac{[(\text{CH}_3)_3]}{[\text{H}]} \times \frac{1}{9} \right] \times 100 \quad (8)$$

$$DM = \left[\frac{[(\text{CH}_3)_2]}{[\text{H}]} \times \frac{1}{6} \right] \times 100 \quad (9)$$

Where $[(\text{CH}_3)_3]$ is the integral of trimethyl amino group at 3.16 ppm.

$[(\text{CH}_3)_2]$ is the integral of dimethyl amino group at 2.89 ppm.

$[\text{H}]$ is the integral of the ^1H peaks between at 4.94 ppm.



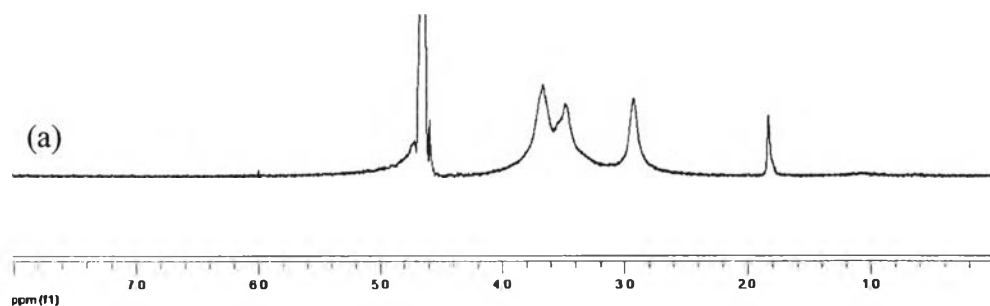


Figure 4.2 The ^1H -NMR spectrum of : (a) chitosan and (b) TMC.

4.2 Characterization of Carboxymethyl Chitosan (CM-chitosan)

4.2.1 Fourier-Transformed Infrared Spectrophotometer (FT-IR)

The FTIR spectrums of chitosan, CM-chitosan-Na salt and CM-chitosan are shown in Fig. 4.3. CM-chitosan (Fig. 4.3c) shows the characteristic absorption peaks of CM-chitosan that are the peak at 1615 cm^{-1} ($-\text{COOH}$), 1093 cm^{-1} ($-\text{C}-\text{O}-$), and 1519 cm^{-1} ($-\text{NH}_3^+$) (Chen *et al.*, 2003, Lu *et al.*, 2007). These were the characteristics of O-CM-chitosan that indicated the $-\text{COOH}$ groups which were introduced at $-\text{OH}$ positions of the native chitosan. Fig. 4.3b is the FTIR spectrum of CM-chitosan-Na. The peak of $-\text{COOH}$ was changed to $-\text{COONa}$ (1592 cm^{-1}), and the $-\text{NH}_3^+$ was changed to $-\text{NH}_2$ (1419 cm^{-1}).

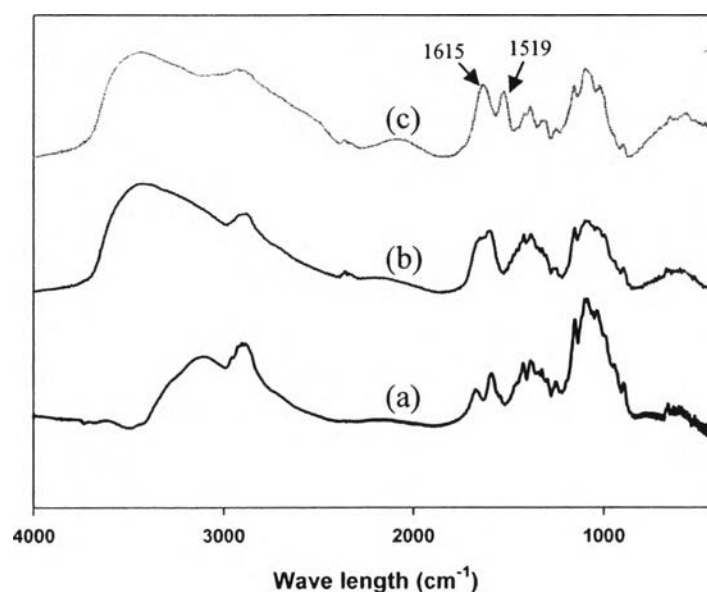


Figure 4.3 The FTIR spectra of : (a) chitosan, (b) CM-chitosan-Na salt and (c) CM-chitosan.

4.2.2 Proton Nuclear Magnetic Resonance Spectrometer ($^1\text{H-NMR}$)

$^1\text{H-NMR}$ spectrometer is used to investigate the functional groups and the structure of CM-chitosan and this instrument can be used to determine the carboxymethylation fraction of the CM-chitosan. Proton assignment of CM-chitosan was (Fig. 4.4a) : $\delta_{1.85} = \text{CH}_3$ (acetyl groups); $\delta_{2.97} = \text{CH}$ (carbon 2 of sugar); $\delta_{3.11} = \text{CH}_2$ (carboxymethyl group on carbon 2 of sugar, $-\text{N-CH}_2\text{-COOD}$); $\delta_{3.30-3.80} = \text{CH} + \text{CH}_2$ (carbon 3-6 of sugar); $\delta_{3.90-4.20} = \text{CH}_2$ (carboxymethyl groups on carbon 3,6 of sugar, $-\text{O-CH}_2\text{-COOD}$); $\delta_{4.21} = \text{CH}_2$ (carboxymethyl groups on carbon 3 of sugar, $-\text{O-CH}_2\text{-COOD}$); $\delta_{4.79-4.94} = \text{CH}$ (carbon 1 of sugar) (Pang *et al.*, 2007 and Lu *et al.*, 2007). The degree of substitution of carboxymethyl groups on primary hydroxyl (C_6), secondary hydroxyl (C_3, O -position), and amino (C_2 , N-position) sites were about 0.55, 0.36, and 0.28, respectively which was calculated according to the following equation (Chen *et al.*, 2003).:

$$f_6 = \frac{1}{2} \frac{(I_d - I_c)}{(I_b + I_g)} \quad (10)$$

$$f_3 = \frac{I_c}{(I_b + I_g)} \quad (11)$$

$$f_2 = \frac{1}{2} \frac{I_f}{(I_b + I_g)} \quad (12)$$

where f_6 is the fractions of carboxymethylation at the position 6-O-

f_3 is the fractions of carboxymethylation at the position 3-O-

f_2 is the fractions of carboxymethylation at the 2-N-

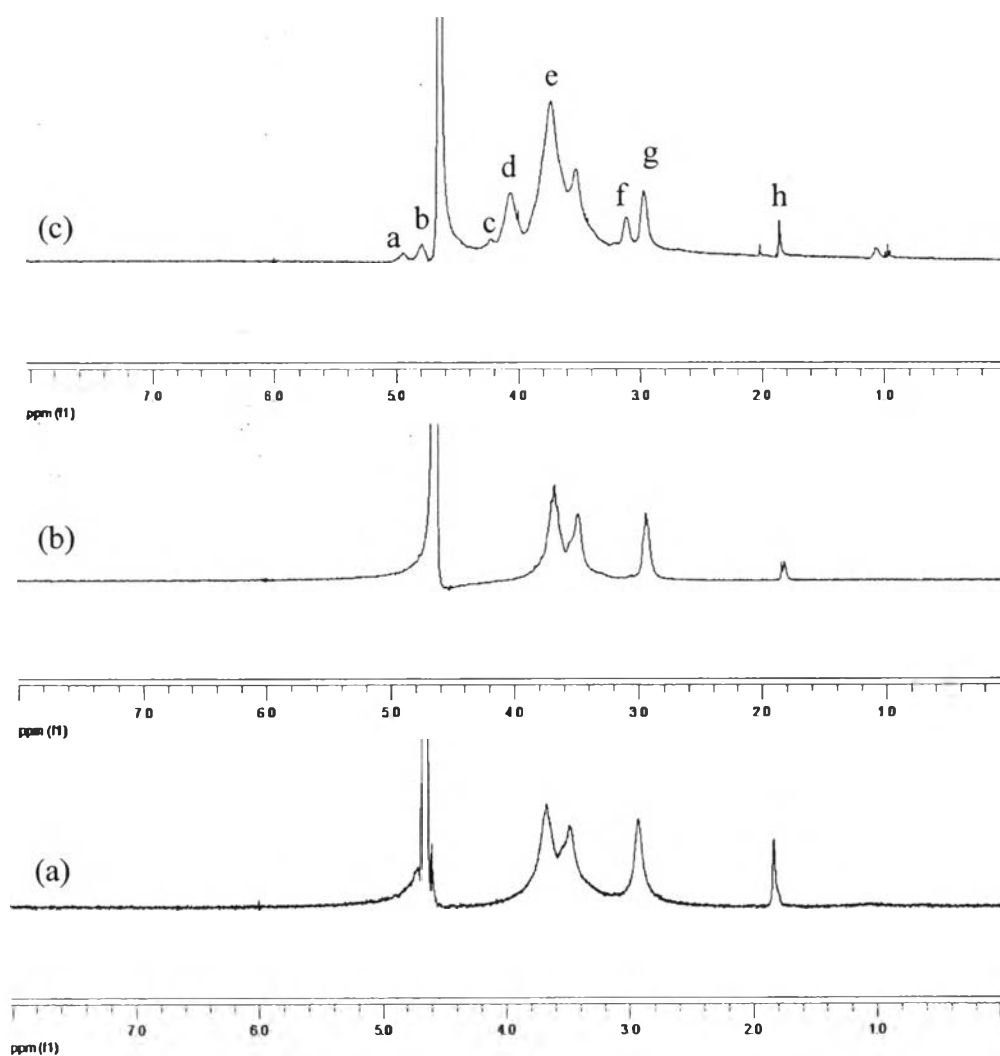


Figure 4.4 The ^1H -NMR spectrum of : (a) chitosan, (b) CM-chitosan-Na salt and (c) CM-chitosan.

4.3 Characterization of the blended hydrogels

4.3.1 Appearance of the Blended Hydrogels

The appearance of the blended hydrogels was shown in Fig. 4.5. The blended hydrogels were prepared by using γ -irradiation technique that was attributed to the homogeneous network structure (Yang *et al.*, 2008). The blended hydrogels at 25 kGy irradiation were not complete hydrogels. They were in a very sticky form of hydrogels. The blended hydrogels were stuck in the nylon bag, that caused by low energy of γ -irradiation. The blended hydrogels at 35 and 45 kGy irradiation were complete hydrogels but these hydrogels had bubbles inside of hydrogels due to high energy of γ -irradiation.

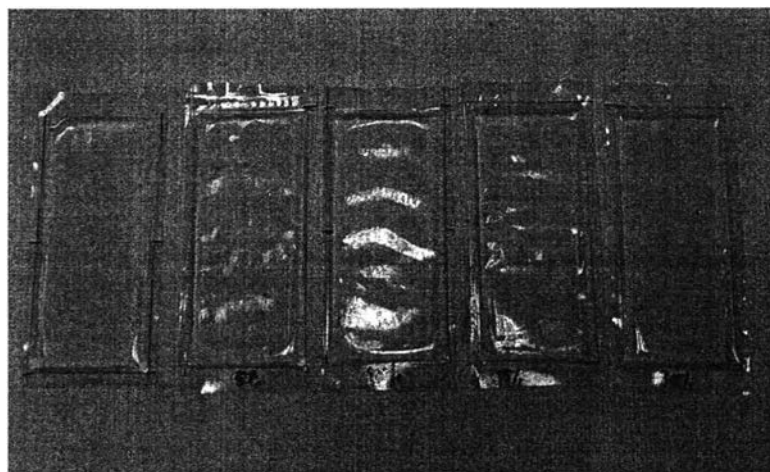


Figure 4.5 The appearance of the blended hydrogels made by γ -irradiation. The compositions of the blended hydrogels were 0, 5, 10, 15, and 20 % CM-chitosan.

4.3.2 Gel Fraction of the Blended Hydrogels

The effect of CM-chitosan content in aqueous solution on the gel fraction of the blended hydrogels at different irradiation doses was also studied. The results were shown in Fig. 4.6. It showed the gel fraction of the blended hydrogels against irradiation doses at various concentration of CM-chitosan (5–20%). Gel fractions of PVA hydrogels was in the range of 89–92%, and gel fractions of the

blended hydrogels containing CM-chitosan were in the range of 79–92%. The gel fraction of the blended hydrogels decreases with increasing the CM-chitosan content while the gel fraction increases with increasing irradiation doses for all blended compositions due to the formation of the blended hydrogels is the cross-linking of PVA molecules. This process was occurred by irradiating of γ -rays, causing radicals in the polymer chains. Those radicals can interact with other chains to form cross-linking network. So, in the systems containing the high irradiation doses will provide more macroradicals than low irradiation doses, resulting in the facilitate cross-linking PVA molecules and hydrogels also have high gel fraction. On the other hand, the high CM-chitosan content provide the low attribution of gel fraction due to CM-chitosan molecules penetrate to PVA networks which prevent intermolecular recombination of PVA molecules leading to low gel fraction. Likewise, the presence of water enhances the mobility of the rigid molecules of polymer allowing macroradicals to recombine with each others when adding CM-chitosan into the PVA hydrogels also decrease gel fraction due to decreasing in water content in the system.

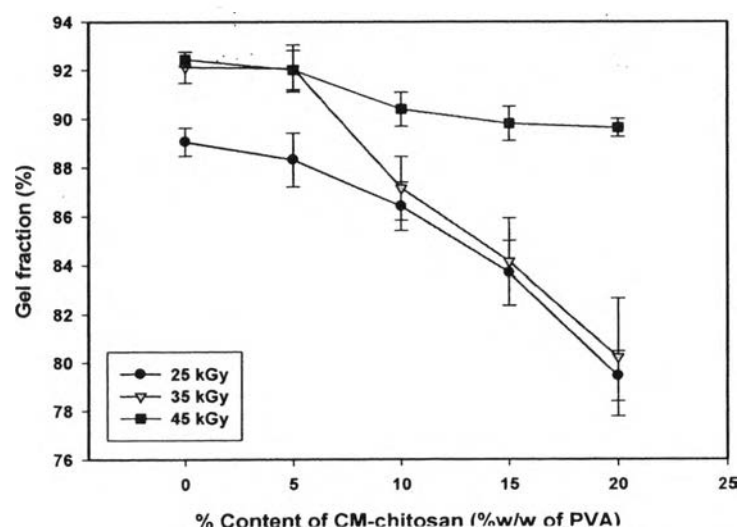


Figure 4.6 The gel fraction of the blended hydrogels as a function of CM-chitosan contents and irradiation doses of γ -rays.

4.3.3 Swelling Behavior of the Blended Hydrogels

The swelling factors of the blended hydrogels are the cross-linking density, the ionic strength of the media, the hydrophilicity of the blended hydrogels and pH of the media, irradiation dose, concentration of polymer, and the temperature of environment. The blended hydrogels were polyelectrolyte complex because the opposite charged groups of CM-chitosan that contains both carboxyl and amino groups, and thus forms a network with oppositely charged structures, occurring a strong electrostatic attraction in the blended network systems and lead to a higher electrostatic force. The degree of swelling of the blended hydrogels with different CM-chitosan content was as a function of γ -irradiation doses. Fig. 4.7 was shown the swelling behavior of the blended hydrogels in distilled water at 48 h. It was found that, the blended hydrogels have the degree of swelling in the range of 199-606%, 189-604%, and 179-482% at 25 kGy, 35 kGy, and 45 kGy respectively. That results indicated the swelling behavior increases with increasing CM-chitosan content due to the hydrophilicity of CM-chitosan (Rosiak *et al.*, 1999). Fig. 4.8 was shown the swelling behavior of the blended hydrogels in SBF pH 7.4 at 48 h. The swelling of the hydrogels showed a typical behavior of polyelectrolyte under ionic strength of SBF solution. It was found that the blended hydrogels have the degree of swelling in the range of 157-307%, 148-292%, and 143-235% at 25 kGy, 35 kGy, and 45 kGy respectively. In this condition the swelling behavior was the same as the swelling behavior in distilled water, but the blended hydrogels in SBF are less swelling than the blended hydrogels in distilled water. Due to SBF consists of many types of ions such as sodium, potassium, magnesium, calcium, and chloride. According to Zhao *et al.*, (2006). they reported the increase of ionic strength in the media led to increasing the osmotic pressure of the media and decreasing the osmotic pressure of the network ions resulted in deswelling of the blended hydrogels. Fig. 4.9 was shown the dimensional swelling of the blended hydrogels (15 %w/w CM-chitosan at 35 kGy) which were immersed in distilled water. The horizontal and vertical dimension of the hydrogels changed about 57 % and 100 % respectively.

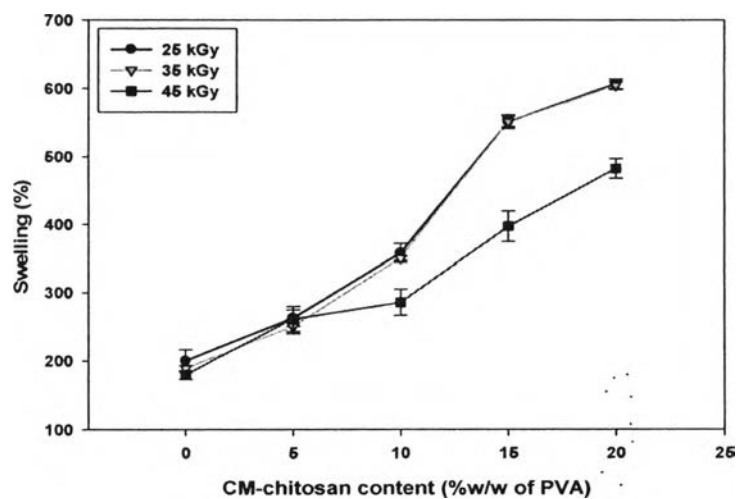


Figure 4.7 The swelling behavior of the blended hydrogels in distilled water at 48 h as a function of CM-chitosan contents and irradiation doses of γ -rays.

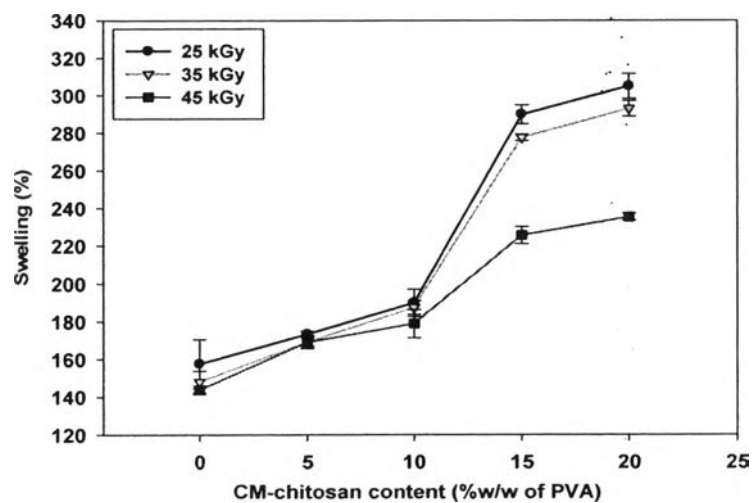


Figure 4.8 The swelling behavior of the blended hydrogels in SBF pH 7.4 at 48 h as a function of CM-chitosan contents and irradiation doses of γ -rays.

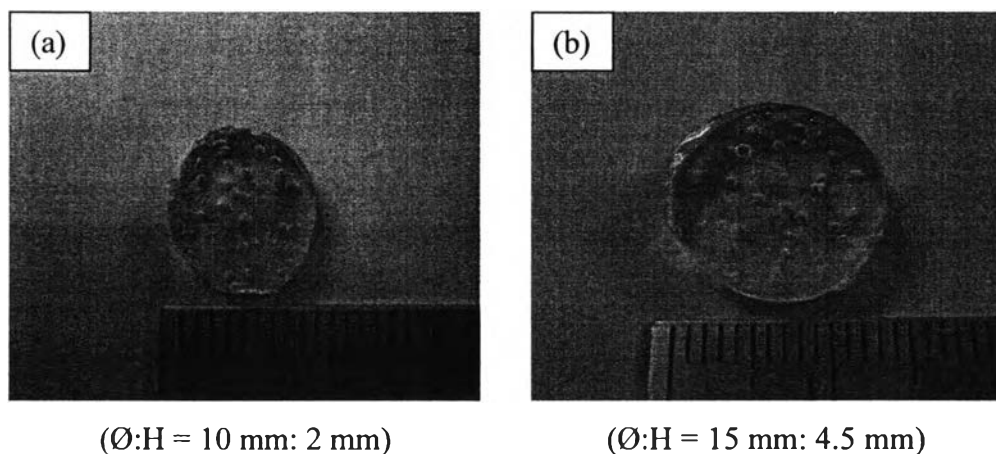


Figure 4.9 The dimensional swelling of the blended hydrogels at 35 kGy, immersed in distilled water : (a) 0 h and (b) 48 h.

4.3.4 Weight Loss of the Blended Hydrogels

The weight loss of the blended hydrogels in distilled water and SBF pH 7.4 solutions with various CM-chitosan content at different irradiation doses which was studied. Fig. 4.10 was represented the weight loss of the blended hydrogels in distilled water at 48 h. It was found that the weight loss of the blended hydrogels in the range of 8-19, 7-17, and 5-8 % at 25, 35, and 45 kGy respectively. Fig. 4.11 was represented the weight loss of the blended hydrogels in SBF pH 7.4 at 48 h. It was found that the weight loss of the blended hydrogels in the range of 4-7, 3-6, and 3-5 % at 25, 35, and 45 kGy respectively. These results indicated the weight loss of the blended hydrogels increases with increasing CM-chitosan content in both condition due to the hydrophilicity of CM-chitosan. On the other hand, the weight loss of the blended hydrogels decreases with increasing the γ -irradiation doses because of the degree of cross-linking network in the blended hydrogels. The weight loss in SBF pH 7.4 is lower than the weight loss in distilled water because SBF is high ionic strength and osmotic pressure led to decrease the osmotic pressure of the network ions resulted in decreasing the solubility of CM-chitosan in the blended hydrogels.

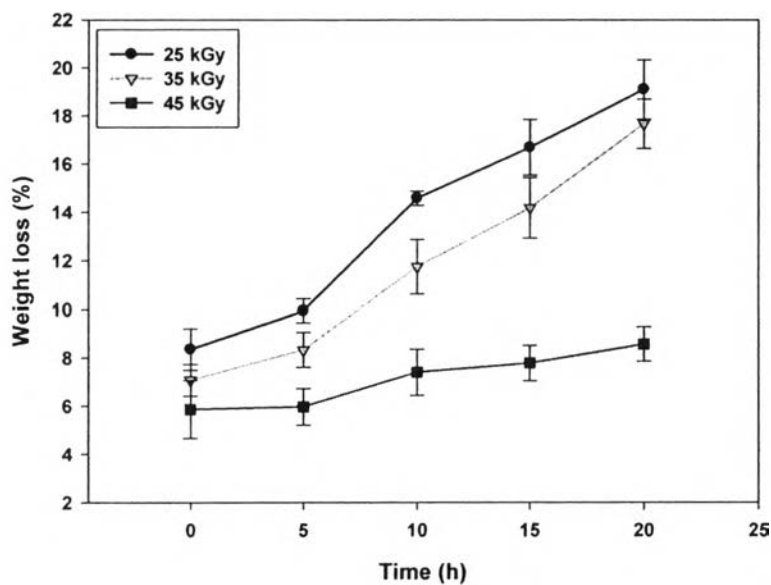


Figure 4.10 The weight loss of the blended hydrogels in distilled water at 48 h as a function of CM-chitosan contents and irradiation doses of γ -rays.

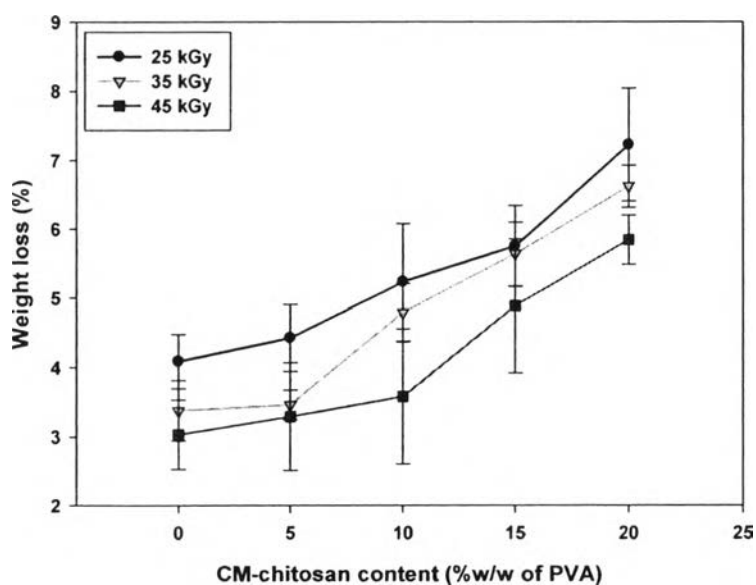


Figure 4.11 The weight loss of the blended hydrogels in SBF pH 7.4 at 48 h as a function of CM-chitosan contents and irradiation doses of γ -rays.

4.3.5 Water Absorption of the Blended Hydrogels

Absorption ability is the requirement of wound dressing, then a good wound dressing should be able to absorb the exudates and toxic components from the wounds surface (Rosiak *et al.*, 1995). Water absorption of the blended hydrogels was studied as a function of CM-chitosan content at different γ -irradiation doses. The results showed in Fig. 4.12, the water absorption increases with increasing the CM-chitosan content due to CM-chitosan and PVA were a water soluble polymer. CM-chitosan could be dissolved in water easier than PVA and the absorption ability could be improved by adding CM-chitosan into PVA hydrogels. On the other hand, water absorption decreased with increasing the irradiation dose. That attributed to an increase in the degree of cross-linking between polymer chains (Salmawi, 2007).

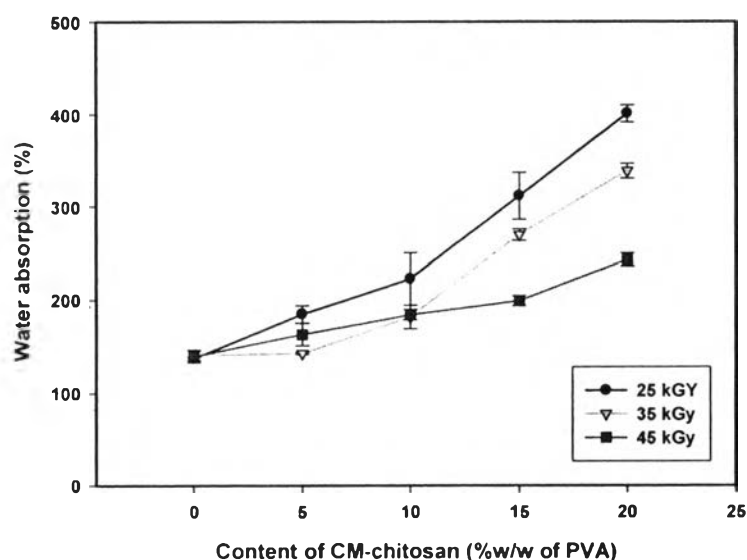


Figure 4.12 The water absorption of the blended hydrogels as a function of CM-chitosan contents and irradiation doses of γ -rays.

4.3.6 Molecular Weight Between Crosslink of the Blended Hydrogels

The molecular weight between crosslink (M_c) of the blended hydrogels with various CM-chitosan content at different irradiation doses was studied. This result was the important parameter for characterizing the crosslinked polymer, which related to the crosslinked density of polymer. M_c was determined by using the equilibrium swelling data. The Flory-Rehner equation. V_1 represented to the

molar volume of water ($18.1 \text{ cm}^3/\text{mol}$ for water) while χ represented to the Flory-Huggins constant ($\chi = 0.494$ for PVA gels and water) (Dhara *et al.*, 1999 and Gudeman *et al.*, 1995). In this work used χ of PVA to calculate M_c of the blended hydrogels. According to Zhao *et al.*, (2003) the irradiation cannot effect on the crosslinking of CM-chitosan in aqueous solutions with concentration lower than 10 %w/v of CM-chitosan. The results were shown in Table 4.1. It was found that the molecular weight between crosslink (M_c) of the blended hydrogels decreased with increasing γ -irradiation doses due to high radicals on the polymer chains and high probability for cross-linking PVA molecules. On the other hand, the molecular weight between crosslink (M_c) of the blended hydrogels increased with CM-chitosan content because CM-chitosan molecules penetrate to PVA networks which prevent intermolecular recombination of PVA molecules. The crosslink density of the blended hydrogels increased with decreasing γ -irradiation doses. On the other hand, the crosslink density of the blended hydrogels decreased with increasing CM-chitosan content. The results can be concluded that the molecular weight between crosslink (M_c) of the blended hydrogels was transverse proportional to the crosslink density of the blended hydrogels.

Table 4.1 Molecular weight between crosslink and the crosslink density of the blended hydrogels

CM-chitosan content (%w/w of PVA)	M_c (g/mol)			V_c ($\times 10^{-21} \text{ ml}^{-1}$)		
	25 kGy	35 kGy	45 kGy	25 kGy	35 kGy	45 kGy
0	33.37	29.75	29.27	2.00	2.25	2.28
5	52.50	42.36	40.22	1.28	1.59	1.68
10	66.45	50.62	43.49	1.02	1.33	1.55
15	163.18	118.89	62.08	0.42	0.57	1.10
20	295.65	201.41	95.41	0.23	0.34	0.72

4.3.7 Moisture Retention Capability of the Blended Hydrogels

Moisture retention capability is an important factor of the wound dressing. The wound dressing should be able to maintain a high humidity at the wound/dressing interface and keep the moisture of the wound (Stashak *et al.*, 2004). The moisture retention capability and water losing rate of the blended hydrogels were studied. The results were shown in Table 4.1 and Table 4.2. Moisture retention capability (R_h) of all blended hydrogels in 6 h is in the rang of 56.1-69.9%. The water losing rate of all blended hydrogels was determined from the slopes of moisture retention capability, that rates were about -5.0×10^{-4} g/min.

Table 4.2 Moisture retention capability of the blended hydrogels at 37 °C for 6 h

CM-chitosan content (%w/w of PVA)	R_h , 6h (%)		
	25 kGy	35 kGy	45 kGy
0	60.65 ± 4.47	66.62 ± 1.32	64.14 ± 1.56
5	56.48 ± 3.35	69.83 ± 1.19	67.14 ± 1.23
10	57.99 ± 3.82	63.62 ± 2.03	64.71 ± 2.19
15	51.94 ± 3.12	69.90 ± 2.69	60.45 ± 4.91
20	56.10 ± 3.92	65.62 ± 2.53	65.39 ± 4.07

(Mean ± S.D. , n = 5)

Table 4.3 Water losing rate of the blended hydrogels at 37 °C for 48 h

CM-chitosan content (%w/w of PVA)	Water losing rate (10^{-4} g/min)		
	25 kGy	35 kGy	45 kGy
0	-5.60	-5.14	-5.35
5	-5.90	-4.84	-5.20
10	-5.77	-5.30	-5.42
15	-6.04	-4.62	-5.74
20	-6.04	-5.18	-5.44

4.3.8 Water Vapor Transmission Rate of the Blend Hydrogels

The water vapor transmission rate (WVTR) is the significant ability of an ideal wound dressing, that wound dressing must be controlled the loss of body fluid and maintain a humidity at the wound surface due to evaporation and exudation are occurred at the wound area (Peppas *et al.*, 1987). The water vapor transmission rate (WVTR) of the blended hydrogels with various CM-chitosan contents at different γ -irradiation doses was investigated. WVTR was represented in Table 4.3. From this table, the results were shown WVTR of the blended hydrogels in the rang of 349–384 , 274-342, and 140-186 gm^2/h at 25, 35 and 45 kGy respectively. The values of WVTR of the blended hydrogels decreased with increasing the γ -irradiation dose that may be attributed to the increasing in the degree of crosslink network. The density hydrogels lead to the water vapor in difficulty to transmit through the hydrogels. The WVTR value must not be high because it will cause a dry condition in the wound area. On the other hand, if the WVTR value is too low, then it will make the accumulation of exudates which may cause the deceleration of healing process and opens up the risk of bacterial growth (Bruin *et al.*, 1990).

Table 4.4 Water vapor transmission rate of the blended hydrogels at 37 °C for 24 h

CM-chitosan content (%w/w of PVA)	Water vapor transmission rate (gm^2/h)		
	25 kGy	35 kGy	45 kGy
0	349.99 ± 21.07	328.81 ± 32.88	140.34 ± 7.21
5	361.94 ± 31.21	286.93 ± 23.93	170.67 ± 17.69
10	384.89 ± 25.57	342.35 ± 38.59	186.00 ± 13.61
15	384.38 ± 28.26	274.30 ± 29.46	175.24 ± 5.32
20	352.36 ± 38.13	292.56 ± 19.46	183.80 ± 14.16

(Mean ± S.D. , n = 5)

4.3.9 Morphology of the Blend Hydrogels

Morphology of the blended hydrogels was investigated by using Scanning Electron Microscope (SEM). The SEM images of cross sections and the

inner surface of the blended hydrogels with different conditions were shown in Table 4.4-4.6. From SEM images, the porosity of the blended hydrogels decreased with increasing CM-chitosan content for the cross section. It was due to an increasing of a polymer mass and a decreasing of the water content in the system. For the inner surface of the blended hydrogels, it is a very small porous structure and very high porosity. The inner surface of the blended hydrogels at 25 and 35 kGy were not different. On the other hand, inner surface at 45 kGy was dense and low porosity due to high energy of irradiation lead to obtaining the high density and the cross-linked network hydrogels.

Table 4.5 Morphology of the blended hydrogels at 25 kGy

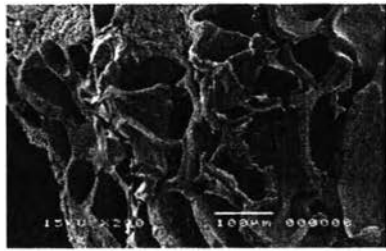
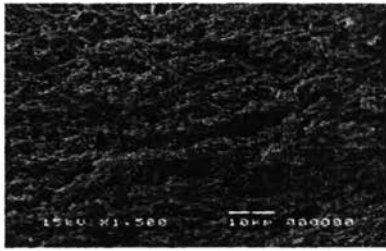
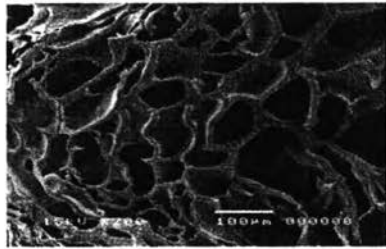
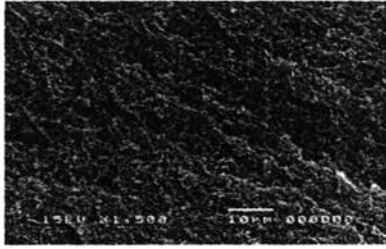
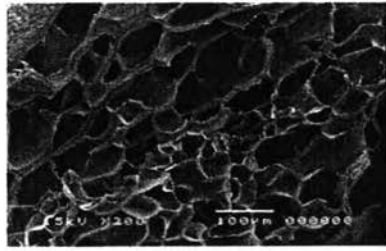
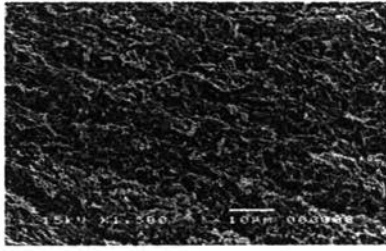
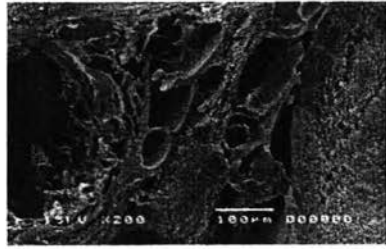
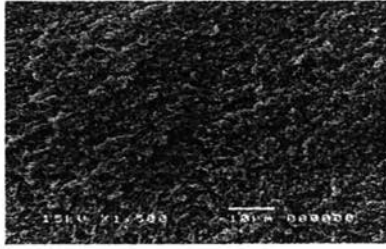
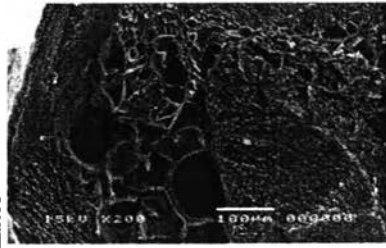
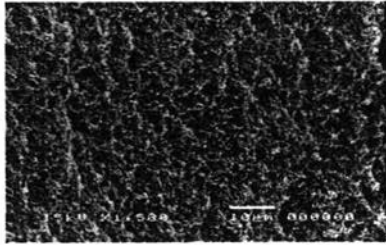
CM-chitosan content (%w/w of PVA)	Magnification = 200X Scale bar = 100µm	Magnification = 1500X Scale bar = 10µm
	Cross section	Inner surface
0		
5		
10		
15		
20		

Table 4.6 Morphology of the blended hydrogels at 35 kGy

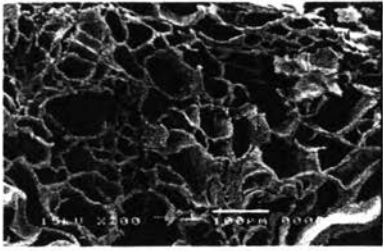
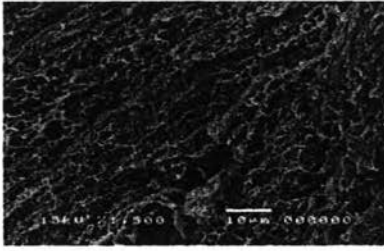
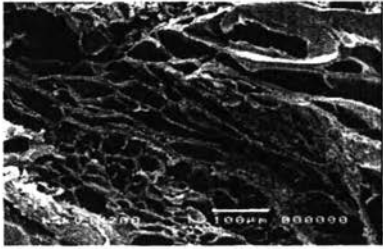
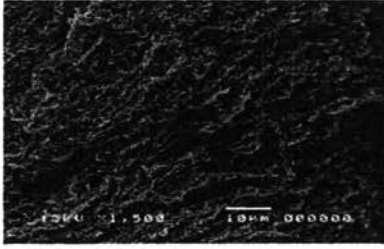
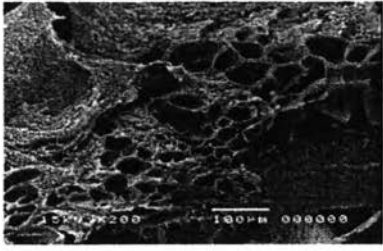
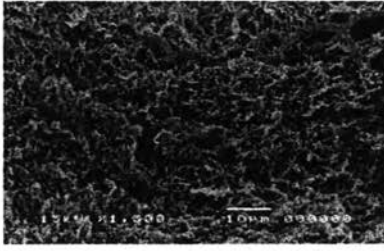
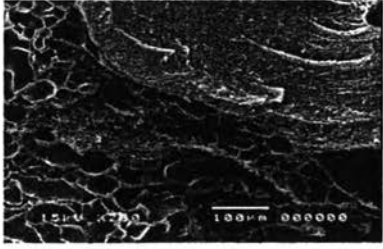
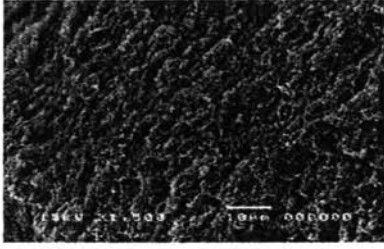
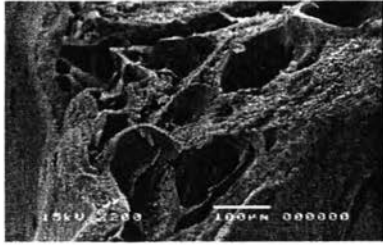

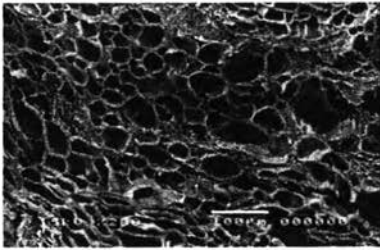
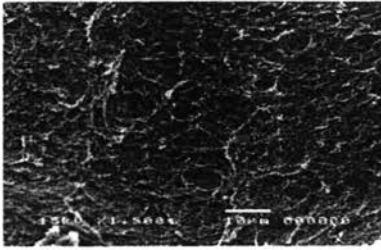
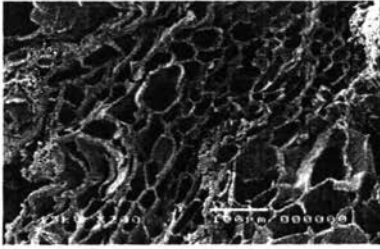
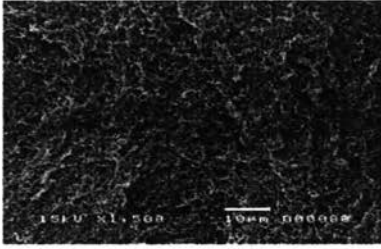
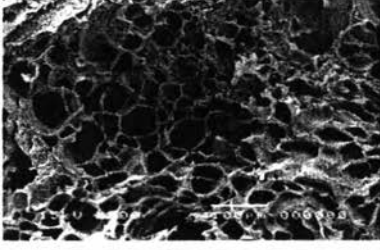
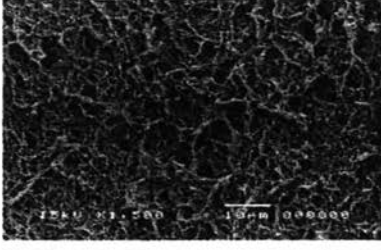
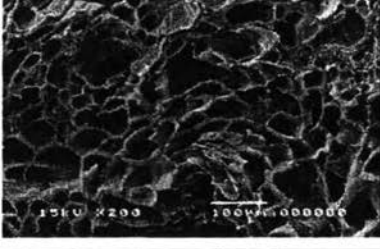
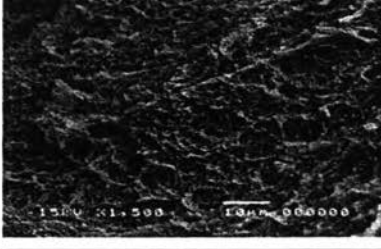
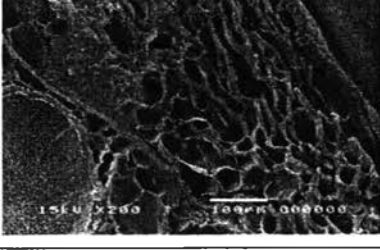
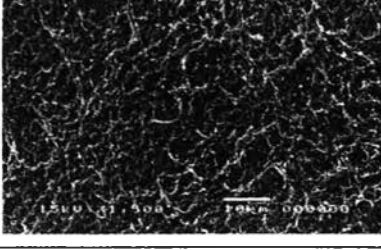
CM-chitosan content (%w/w of PVA)	Magnification = 200X Scale bar = 100 μ m	Magnification = 1500X Scale bar = 10 μ m
	Cross section	Inner surface
0		
5		
10		
15		
20		

Table 4.7 Morphology of the blended hydrogels at 45 kGy

CM-chitosan content (%w/w of PVA)	Magnification = 200X Scale bar = 100 μ m	Magnification = 1500X Scale bar = 10 μ m
	Cross section	Inner surface
0		
5		
10		
15		
20		

4.4 Antibacterial Activity Assay

4.4.1 Minimum Inhibitory Concentration (MIC) of TMC and CM-chitosan

After changing chitosan to TMC and CM-chitosan, it made to water soluble polymer with a high charge density. TMC and CM-chitosan are the antibacterial polymers, which have been widely used in medical applications. The minimum inhibitory concentration (MIC) is the lowest concentration of antibacterial activity that can inhibit the growth of bacteria after overnight incubation (Goy *et al.*, 2009). In this studied, the antibacterial activity of TMC and CM-chitosan against bacteria in skin infection was performed by agar method. The tested bacteria were consisted of *Acinetobacter lwoffii* ATCC 15309 and *Escherichia coli* ATCC 25922 which are Gram-negative bacteria and *Staphylococcus aureus* ATCC 25923, *Staphylococcus aureus* DMST 20654 (MRSA), *Staphylococcus epidermidis* ATCC 12228, and *Listeria monocytogenes* DMST 17303 which are Gram-positive bacteria. Gram-negative and Gram-positive bacteria have the different cell walls (Sun *et al.*, 2006). Gram-negative bacteria, its cell wall is bilayer structure that layers are made up of the thin membrane of peptide polyglycogen and outer membrane consists of lipopolysaccharide, lipoprotein and phospholipids. Gram-positive bacterium, its cell wall is the peptide polyglycogen. The antibacterial mechanisms of TMC, the positive charge of TMC at C-2 lead to a polycationic which can interact with an anionic charges of microorganisms on membrane which leads to leakage of protienaceous and other intracellular components. The penetration of TMC into the nuclei of the microorganisms can lead TMC to binds with DNA and inhibits the synthesis of mRNA and proteins (Shahidi *et al.*, 1999). On the other hand, CM-chitosan has carboxymethyl groups and ammonium groups along the chain that can occur the chelation of metals, suppression of spore elements and binding to essential nutrients which cause to inhibit the production of toxins and microbial growth. These are the causative of cell death (Shahidi *et al.*, 1999 and Goy *et al.*, 2009). Table 4.7 and 4.8 were shown the MIC of TMC and CM-chitosan, respectively. The results showed, that MIC values of TMC against Gram-negative bacteria were inhibited at 1.25-2.5 mg/ml and inhibited at 2.5-5 mg/ml for Gram-positive bacteria. TMC showed the inhibition activity of Gram-negative bacteria was better than Gram-positive bacteria.

The similar results were obtained with CM-chitosan that MIC values against Gram-negative bacteria were inhibited at 1.25-2.5 mg/ml, but its were inhibited Gram-positive bacteria at 1.25-2.5 mg/ml. The inhibition activity of Gram-positive bacteria of CM-chitosan was better than TMC.

Table 4.8 MIC of TMC aginst bacteria in skin infection

Bacteria	MIC (mg/ml)
<i>Acinetobacter Iwoffii</i> ATCC 15309	1.25
<i>Escherichia coli</i> ATCC 25922	2.50
<i>Staphylococcus aureus</i> ATCC 25923	5.00
<i>Staphylococcus aureus</i> DMST 20654 (MRSA)	2.50
<i>Staphylococcus epidermidis</i> ATCC 12228	2.50
<i>Listeria monocytogenes</i> DMST 17303	2.50

Table 4.9 MIC of CM-chitosan aginst bacteria in skin infection

Bacteria	MIC (mg/ml)
<i>Acinetobacter Iwoffii</i> ATCC 15309	1.25
<i>Escherichia coli</i> ATCC 25922	2.50
<i>Staphylococcus aureus</i> ATCC 25923	2.50
<i>Staphylococcus aureus</i> DMST 20654 (MRSA)	2.50
<i>Staphylococcus epidermidis</i> ATCC 12228	1.25
<i>Listeria monocytogenes</i> DMST 17303	2.50

Note : In this study, it did not investigate MIC of chitosan because the acetic acid solution that is the solvent for dissolved chitosan, and it is toxic to bacteria.

4.4.2 Colony Count Method

From all properties of the blended hydrogels, it was found that blended hydrogel containing 15% of CM-chitosan is a suitable hydrogels for wound dressing application due to it has lower water losing rate and higher moisture

retention capability. These are an important properties of the wound dressing. The aim of this research is the improving of antibacterial activity of the PVA hydrogels that hydrogels containing 15% of CM-chitosan and 5-15% of TMC were tested against *Acinetobacter lwoffii* ATCC 15309, *Escherichia coli* ATCC 25922, Gram-positive *Staphylococcus aureus* ATCC 25923, *Staphylococcus aureus* DMST 20654 (MRSA), *Staphylococcus epidermidis* ATCC 12228, and *Listeria monocytogenes* DMST 17303 by colony count method. The PVA hydrogels were used as the negative control. The colony forming unit per ml (CFU/ml) of the blended hydrogels is showed in Fig. 4.13. It was found that, CFU values of *Acinetobacter lwoffii* ATCC 15309 and *Staphylococcus epidermidis* ATCC 12228 had on the bacterial colonies did not appear on the agar plate. For *Escherichia coli* ATCC 25922, *Staphylococcus aureus* ATCC 25923, *Staphylococcus aureus* DMST 20654, and *Listeria monocytogenes* DMST, it was found that CFU values decrease with increasing TMC content. It implied that high TMC molecules, increases high positively charges lead to increases antibacterial activity. The bacterial reduction rate (BRR) of the blended hydrogels is shown in Fig. 4.14. According to Fig. 4.14, the BRR values of the 15% CM-chitosan hydrogels containing 5-10% of TMC against *Acinetobacter lwoffii* ATCC 15309, *Escherichia coli* ATCC 25922, *Staphylococcus aureus* ATCC 25923, *Staphylococcus aureus* DMST 20654 (MRSA), *Staphylococcus epidermidis* ATCC 12228, and *Listeria monocytogenes* DMST 17303 were about 99.99 %, 3.25-99 %, 46.08-99.05 %, 2.20-99.96 %, 99.96-100 %, and 99.99 % respectively. The results confirmed that the blended hydrogels can be used as antibacterial wound dressing.

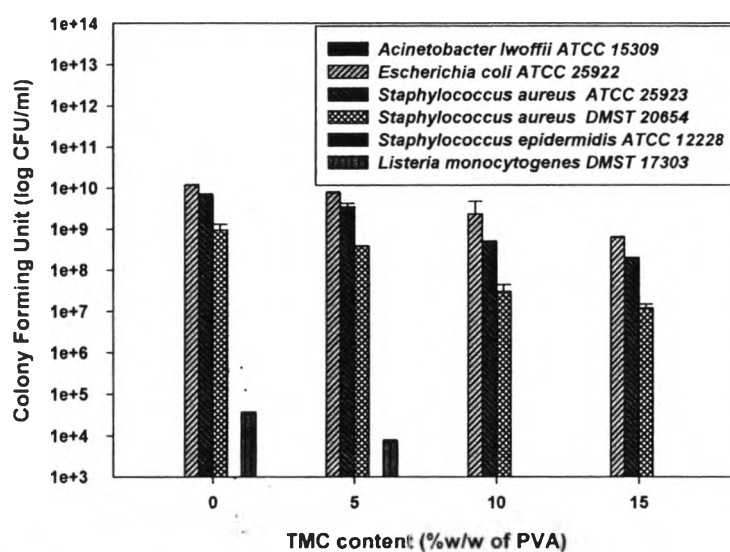


Figure 4.13 The colony forming unit of the blended hydrogels.

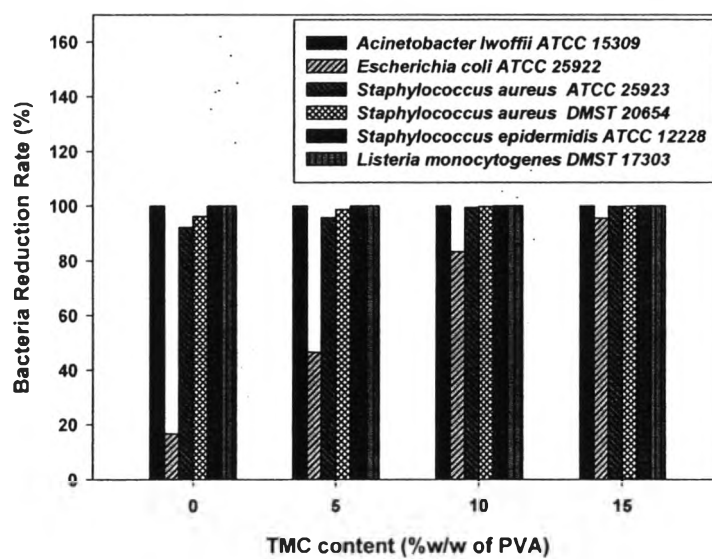


Figure 4.14 The bacteria reduction rate of the blended hydrogels.

4.5 Cytotoxicity of the Blended Hydrogels

4.5.1 Indirect Cytotoxic Assay

The most consideration of the material to use as the wound dressing is a toxicity of the material. Thus, the toxicity of the blended hydrogels must be tested to certify materials. Toxicity of the blended hydrogels were investigated via indirect cytotoxicity technique by using L929 cells and using MTT assay to determine the number of relative cell viability. In this work, there are 2 types of the blended hydrogels which are PVA/CM-chitosan hydrogels and PVA/CM-chitosan/TMC hydrogels. Fig.4.15 showed percent viability of L929 cells of PVA/CM-chitosan hydrogels. The results showed that the relative cell viability of all conditions is more than the relative cell viability of control at all periods. This results similarly to relative cell viability of PVA/CM-chitosan/TMC hydrogels (Fig. 4.16). All of these results showed that released CM and TMC substances were not harmful to L929 cells, and these hydrogels may encouraged the proliferation of cells. Therefore, the fabricated hydrogels can be used as a wound dressing for medical application.

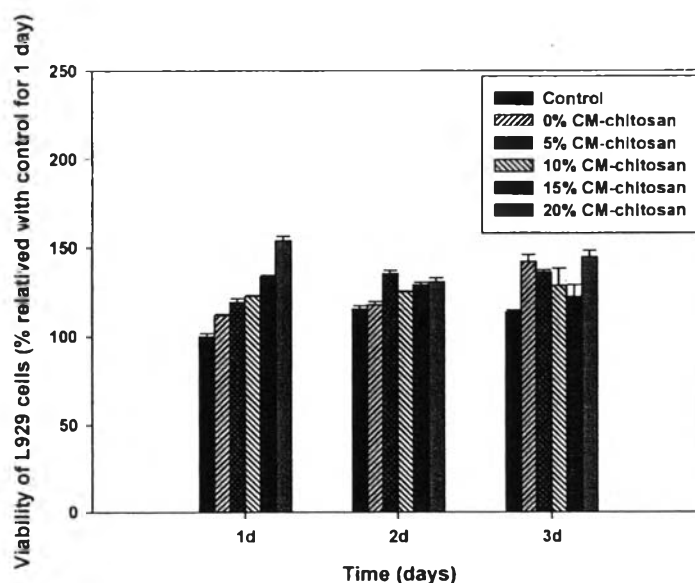


Figure 4.15 Indirect cytotoxic evaluation of the PVA/CM-chitosan hydrogels based on the viability of L 929 cultured with a serum-free medium containing DMEM for 1, 2 and 3 days.

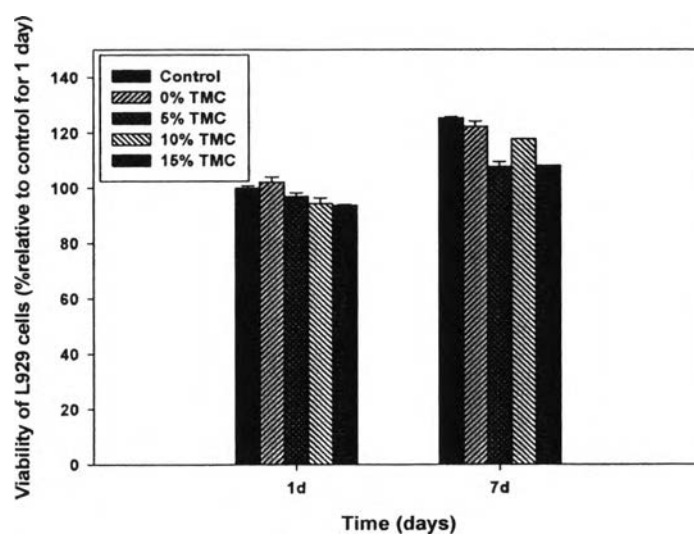


Figure 4.16 Indirect cytotoxic evaluation of the PVA/CM-chitosan/TMC hydrogels based on the viability of L 929 cultured with a serum-free medium containing DMEM for 1 and 7 days.